Received 18 January 2022
Revised 21 February 2022
Accepted 6 April 2022

Seismic response of the long-span steel truss arch bridge with the thrust under multidimensional excitation

Yongliang Zhang, Jibei Ma, Xingchong Chen and Yun Wang
School of Civil Engineering, Lanzhou Jiaotong University, Lanzhou, China

Abstract

Purpose – Under different ground motion excitation modes, the spatial coupling effect of seismic response for the arch bridge with thrust, seismic weak parts and the internal force components of the control section of main arch ribs are analyzed.

Design/methodology/approach – Taking a 490 m deck type railway steel truss arch bridge as the background, the dynamic calculation model of the whole bridge was established by SAP2000 software. The seismic response analyses under one-, two- and three-dimension (1D, 2D and 3D) uniform ground motion excitations were carried out.

Findings – For the steel truss arch bridge composed of multiple arch ribs, any single direction ground motion excitation will cause large axial force in the chord of arch rib. The axial force caused by transverse and vertical ground motion excitation in the chord of arch crown area is 1.4–3.6 times of the corresponding axial force under longitudinal seismic excitation. The in-plane bending moment caused by the lower chord at the vault is 4.2–5.5 times of the corresponding bending moment under the longitudinal seismic excitation. For the bottom chord of arch rib, the arch foot is the weak part of earthquake resistance, but for the upper chord of arch rib, the arch foot, arch crown and the intersection of column and upper chord can all be the potential earthquake-resistant weak parts. The normal stress of the bottom chord of the arch rib under multidimensional excitation is mainly caused by the axial force, but the normal stress of the upper chord of the arch rib is caused by the axial force, in-plane and out of plane bending moment.

Originality/value – The research provides specific suggestions for ground motion excitation mode and also provides reference information for the earthquake-resistant weak part and seismic design of long-span deck type railway steel truss arch bridges.

Keywords Railway steel truss arch bridge, Seismic response, Multidimensional excitation, Spatial coupling effect, Internal force component

Paper type Research paper

1. Introduction

Earthquake is highly random. When an earthquake occurs, both the magnitude and the direction are random (Su & Chen, 2008). In the process of seismic response analysis, the most unfavorable direction should be selected to apply ground motion (Wang & Li, 2007). Fan (1990) and Li *et al.* (2015) point out that the ground motion during earthquake is a complex multidimensional motion, including three translation components and three rotational components, which is verified by both theoretical research and earthquake damage

This research was supported by the National Natural Science Foundation of China (Grant No. 51768037) and "Foundation of A Hundred Youth Talents Training Program of Lanzhou Jiaotong University." On behalf of all authors, the corresponding author states that there is no conflict of interest.

Railway Sciences
Vol. 1 No. 1, 2022
pp. 40-55
Emerald Publishing Limited
e-ISSN: 2755-0915
p-ISSN: 2755-0907
DOI 10.1108/RS-04-2022-0005

experience. At present, there are few observation data of seismic rotational components, which cannot be considered in seismic response analysis. The structure of long-span arch bridge is complex, and its dynamic characteristics have certain spatial coupling characteristics. Not only 1D seismic action but also combined action of multidimensional ground motions should be considered in seismic response analysis.

Many results have been achieved in the research about the impact of ground motion excitation mode on seismic response of arch bridge. Luo Zhu, & Yu. (2019) and Peng Zhu, & Zang. (2009) analyzed the seismic response characteristics of deck type simple system reinforced concrete arch bridge, through type concrete filled steel tube rigid frame tied-arch bridge and reinforced concrete box plate arch bridge by adopting four different ground motion excitation modes (independent and simultaneous input in longitudinal, transverse and vertical directions). Chen and Guo (2010) analyzed the impact of traveling wave effect on the seismic response of Chongqing Chaotianmen Yangtze River Bridge (half-through continuous steel truss tied-arch bridge) by adopting the unidirectional and bidirectional ground motion input modes. Literature Xia and Zhong (2009) analyzed the seismic response of Nanjing Dashengguan Bridge under uniform excitation by adopting the combination mode of ground motion excitation in Eurocode (Eurocode 8, 2005). Li *et al.* (2020) took the half-through steel arch bridge as the research object and analyzed the damage development of steel arch bridge under longitudinal + vertical, longitudinal + transverse + vertical ground motion input. Zhuge *et al.* (2019) took a deck type steel truss arch bridge as the research object, and analyzed the damage state of long-span steel arch bridge under longitudinal transverse and bidirectional (transverse + longitudinal) ground motion input. Liang and Chen (2009) studied the impact of geometric nonlinearity and material nonlinearity on the seismic response of a deck type two-hinge steel arch bridge. According to existing literature, most of the research objects focus on reinforced concrete arch bridge or zero-thrust arch bridge of beam-arch combination type and other types, and mainly studied the damage mechanism of steel truss arch bridge after nonlinearity of structural member strength. However, there are few research studies on the mechanical characteristics of the seismic response of long-span deck type steel truss arch bridge with complex structure, numerous chord members, dense vibration modes and obvious spatial seismic response coupling, that is, the spatial coupling effect and the distribution characteristics of internal force components of arch rib.

In this paper, a 490 m long-span deck type railway steel truss arch bridge was taken as the research object, and SAP2000 software was used to study the seismic response of long-span steel truss arch bridge under one-, two- and three-dimension (1D, 2D and 3D) ground motion excitation.

2. Engineering background and dynamic calculation model of the whole bridge

The deck type steel truss arch bridge of a railway, as shown in Figure 1, has a span of 490 m. The catenary with the arch axis coefficient of 2.0 is adopted for the arch axis, and the rise-span ratio is 1/4.475. The arch rib is of basket-handle arch structure, with an inward inclination of 3.65°. Four truss arches are designed, every two of which constitutes one rib, and the center distance of two main trusses of each rib is 3.4 m. The arch ribs are connected into a whole through cross struts. The center distance of two arch ribs is 32 m at the arch foot and 18 m at the arch crown. Truss arch adopts variable truss height. The truss height of arch crown is 11 m and that of arch foot is 16 m. The upper and lower chords are subject to box section, and both the beam height and width are 2.0 m. The main arch ring and web member are made of Q370q steel, the main truss connection system is made of Q345q steel, the spandrel column and steel box girder are made of Q345q steel and reinforced concrete bridge pier is adopted as junction pier. Separated embedded foundation is adopted for the arch abutment of main bridge. The engineering site in the bridge site area is classified as Class II.

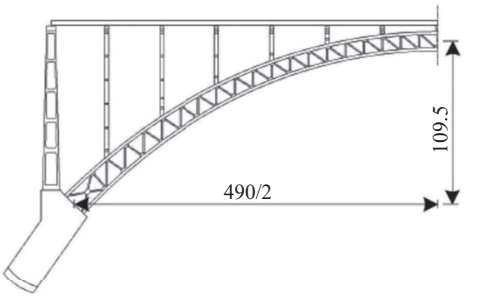

Elevation of half-bridge

(a)

Section at arch crown of 1/2 arch ring section at arch foot of 1/2 arch ring

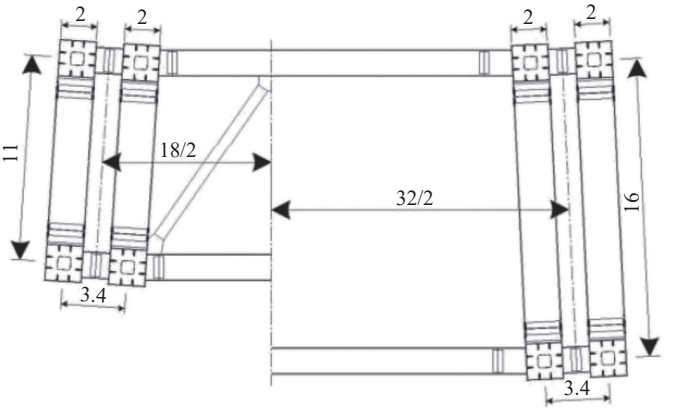

Cross section of main truss

(b)

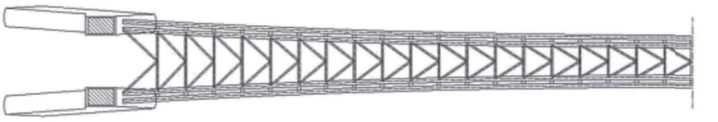

Plan of half-bridge

(c)

Figure 1.
Structural layout of long-span steel truss arch bridge (unit: m)

The peak acceleration of ground motion is 0.248 *g* (*g* is gravity acceleration), and the period of ground motion response spectrum is 0.45 s.

According to the structural characteristics of the bridge, the finite element software SAP2000 is adopted to establish the finite element model of the whole bridge, as shown in Figure 2. The main arch rib, spandrel column, steel box girder and junction pier are all simulated by spatial beam element. The bearings set between the spandrel column and the main beam and between the junction pier and the main beam are simulated by coupling of degrees of freedom, and both the junction pier bottom and arch foot are consolidated. The model has a total of 1,040 nodes and 2,060 elements.

According to the site characteristics of the bridge site area, representative EL-centro wave (the peak acceleration is 341.7 cm s^{-2} and the site characteristic period is 0.55 s) and Taft wave (the peak acceleration is 175.9 cm s^{-2}, and the site characteristic period is 0.44 s) are selected from the Pacific Earthquake Engineering Research Center (PEER website) as the ground motion input in longitudinal, transverse and vertical directions. The peak values of EL-centro and Taft waves are all adjusted to 0.248 *g*, and the acceleration time history of EL-centro and Taft waves after amplitude modulation is shown in Figures 3 and 4.

3. Spatial coupling of seismic response of long-span deck type steel arch bridge

1D ground motion excitation is considered and fed as input in longitudinal, transverse and vertical directions, respectively, for the seismic response analysis of long-span steel truss arch bridge under uniform excitation. For the convenience of expressing the spatial coupling characteristics of structural internal force, the spatial coupling coefficient of structural internal force is introduced for dimensionless treatment of structural internal force. When the axial force and in-plane bending moment are discussed, the spatial coupling coefficient is defined as the ratio of the maximum absolute value of internal force caused by transverse or vertical input to the maximum absolute value of internal force caused by longitudinal input; when out-of-plane bending moment is discussed, the spatial coupling coefficient is defined as the ratio of the maximum absolute value of internal force caused by longitudinal or vertical input to the maximum absolute value of internal force caused by transverse input. Under unidirectional ground motion excitation, due to the symmetry of the structure, the maximum absolute value of the structural response also satisfies the symmetry. Under the excitation of

Figure 2.
Dynamic calculation model of the whole bridge

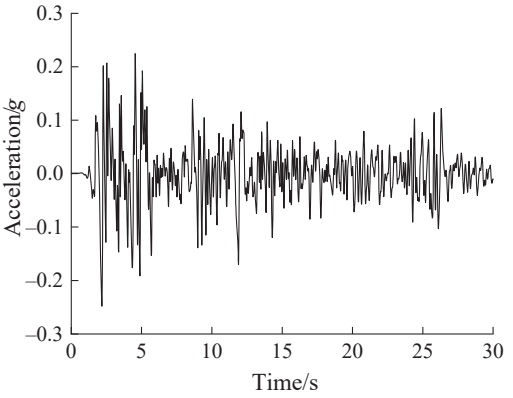

Figure 3.
Acceleration time history of EL-centro wave

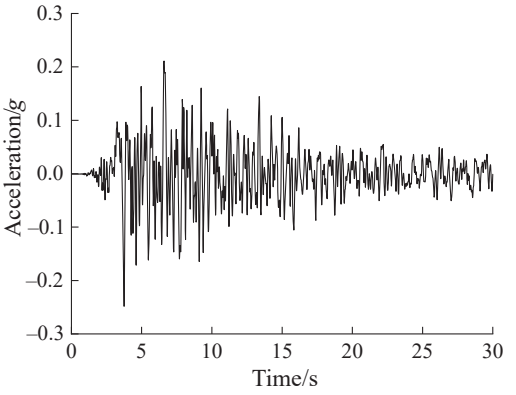

Figure 4.
Acceleration time history of Taft wave

EL-centro wave and Taft wave, the analysis results of internal force spatial coupling coefficient of upper and lower chords of arch rib are shown in Tables 1 and 2 respectively.

According to the analysis results in Tables 1 and 2, the following conclusions can be drawn.

Table 1.
Spatial coupling coefficient of structural internal force under EL-centro wave excitation

Internal force of section	Ground motion input direction	Spatial coupling coefficient of internal force of upper chord of arch rib			Spatial coupling coefficient of internal force of lower chord of arch rib		
		Left arch foot	1/4 span	Arch crown	Left arch foot	1/4 span	Arch crown
Axial force	Transverse	0.24	0.42	1.53	0.66	0.42	2.00
	Vertical	0.16	0.88	1.40	0.81	0.33	2.73
In-plane Bending moment	Transverse	0.37	0.26	0.07	0.91	0.33	4.26
	Vertical	0.29	0.32	0.08	0.43	0.55	4.64
Out-of-plane Bending moment	Longitudinal	0.07	0.11	0.94	0.02	0.12	0.13
	Vertical	0.02	0.11	0.04	0.01	0.04	0.42

Table 2.
Spatial coupling coefficient of structural internal force under Taft wave excitation

Internal force of section	Ground motion input direction	Spatial coupling coefficient of internal force of upper chord of arch rib			Spatial coupling coefficient of internal force of lower chord of arch rib		
		Left arch foot	1/4 span	Arch crown	Left arch foot	1/4 span	Arch crown
Axial force	Transverse	0.50	0.47	2.26	0.92	0.42	2.23
	Vertical	0.23	1.25	2.06	1.37	0.44	3.59
In-plane Bending moment	Transverse	0.50	0.25	0.10	0.84	0.43	5.35
	Vertical	0.39	0.37	0.10	0.62	0.81	5.50
Out-of-plane Bending moment	Longitudinal	0.02	0.08	0.04	0.02	0.05	0.43
	Vertical	0.06	0.06	1.06	0.02	0.10	0.10

(1) For the steel truss arch bridge composed of multiple arch ribs, any unidirectional ground motion excitation will cause large axial force in the chord of arch rib, and the axial force coupling of the chord of arch rib is obvious and also inevitable. There are two reasons: (1) Under longitudinal and vertical ground motion excitation, the arch rib will generate in-plane vibration, while the arch bridge is of the structure with thrust in plane, and axial force will inevitably be caused in the chord of arch rib. (2) Multi-arch rib steel truss arch bridge can be regarded as a multi-arch rib curved truss structure fixed at the arch foot in the transverse direction of bridge. Under the transverse ground motion excitation, the arch rib will occur transverse inclined deformation, and the chord of arch rib will cause axial force due to the frame effect (Zhao & Zhou, 2006, 2007).

(2) The axial force caused by transverse and vertical ground motion excitation in the chord of arch crown area is 1.4–3.6 times of the corresponding axial force under longitudinal ground motion excitation. This is because that both transverse and vertical ground motion excitation can excite the positive symmetric vibration mode of the structure; meanwhile, the axial force is the internal force of the positive symmetric structure, so the axial force of the chord at the arch crown is significantly increased, while the longitudinal ground motion excitation can only excite the anti-symmetric vibration mode. Therefore, the axial force caused at the arch crown is small.

(3) The in-plane bending moment caused by transverse and vertical ground motion excitation at the lower chord of arch crown is 4.2–5.5 times of the corresponding bending moment under longitudinal ground motion excitation. Except the arch crown area, the out-of-plane bending moment value caused by longitudinal and vertical ground motion excitation to the chord of arch rib is small.

(4) There is basically no horizontal coupling of ordinary straight beam bridge, but the spatial coupling of seismic response of long-span complex steel truss arch bridge is remarkable, which makes the seismic response of the structure more complex.

4. The most unfavorable ground motion excitation mode and seismic response characteristics of the long-span deck type steel truss arch bridge

Due to the randomness of ground motion in time and space, that is, the spatial characteristics of ground motion, it is not enough to only consider the 1D earthquake action, but needed to consider the simultaneous action of multidimensional ground motion, so as to determine the maximum seismic response caused by the structure of long-span bridge. For the selection of ground motion, the records of safety assessment of ground motion or strong earthquake can be used. For the seismic design of long-span and complex bridge, the seismic department usually provides the safety assessment report of ground motion at the bridge site, and several safety assessment acceleration time history records with different probability of exceedance are provided in the report. The acceleration time history records are the records of horizontal direction. As for the ground motion excitation mode, the *Code for Seismic Design of Railway Engineering (GB 50111-2006)* stipulates that 65% of horizontal ground motion can be used for dynamic analysis of vertical seismic action. However, the actual ground motion records are very complex, and the recorded longitudinal, transverse and vertical ground motion intensities and waveform are different under different magnitudes, epicentral distances and site conditions. Considering relevant provisions in *Code for Seismic Design of Buildings (GB 50011-2010)*, this paper assumes that the seismic waves input along the longitudinal, transverse and vertical directions of the bridge are all the same wave, and only the peak value is adjusted to analyze the impact of 1D, 2D and 3D ground motion excitation on the seismic

response of steel truss arch bridge. Among them, 1D ground motion excitation mode is to input seismic waves along the longitudinal direction (X direction) and transverse direction (Y direction) of the bridge respectively; 2D ground motion excitation mode is to input seismic waves along X direction and Z direction or Y direction and Z direction simultaneously (Z direction refers to vertical direction); 3D ground motion excitation mode is to input seismic waves along X direction, Y direction and Z direction simultaneously. Table 3 is the specific ground motion excitation modes and combinations (Chen & Xia, 2018).

When EL-centro wave and Taft wave are input, the calculation results of the two waves are similar, so only the calculation results of EL-centro wave are given. When EL-centro wave is input, the envelope diagram of the maximum internal force of the upper and lower chords of arch rib under different ground motion excitation modes is as shown in Figures 5–10. For the convenience of expressing the influence law of the most unfavorable seismic response of the upper and lower chords of arch rib, the calculation results of the internal force ratio of the upper and lower chord control section of arch rib are given in two groups, as shown in Tables 4 and 5. The internal force ratio is defined as the ratio of the maximum internal force under 1D and 2D excitation to the maximum internal force under 3D excitation.

The following results can be seen in Figure 5–10, Tables 4 and 5.

(1) The in-plane bending moment under X-direction ground motion excitation and the out-of-plane bending moment under Y-direction ground motion excitation of the upper chord of arch rib present obvious multi-peak distribution characteristics along the longitudinal direction of arch rib, and each peak point of bending moment corresponds to the position of the column. Both the maximum in-plane and out-of-

Table 3.
Input mode and combination of ground motion

Case	Excitation mode	Combination
1	Longitudinal	X
2	Longitudinal + Vertical	$X + 0.65Z$
3	Longitudinal + Transverse + Vertical	$X + 0.85Y + 0.65Z$
4	Transverse	Y
5	Transverse + Vertical	$Y + 0.65Z$
6	Transverse + Longitudinal + Vertical	$Y + 0.85X + 0.65Z$

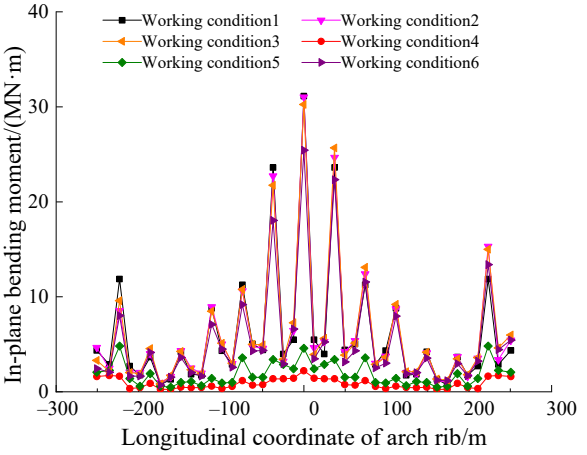

Figure 5.
In-plane bending moment of upper chord of arch rib

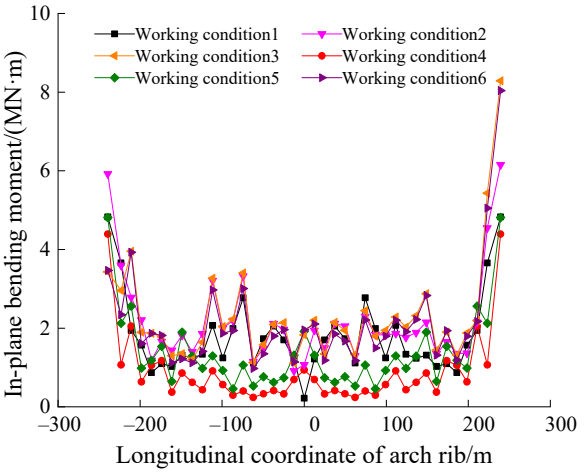

Figure 6.
In-plane bending moment of lower chord of arch rib

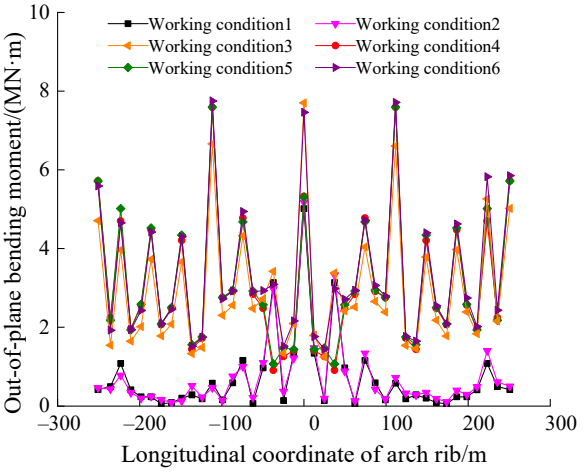

Figure 7.
Out-of-plane bending moment of upper chord of arch rib

plane bending moments of the upper chord of arch rib occur at the arch crown. However, both the maximum in-plane and out-of-plane bending moments of the lower chord of arch rib occur at the arch foot, and the value is obviously larger than that of other parts of arch rib.

(2) For the lower chord of arch rib, both the axial force and bending moment of arch foot section are obviously larger than those of other parts, so the arch foot is an earthquake-resistant weak part. However, for the upper chord of arch rib, the internal forces at the arch foot, the arch crown and the intersection between the column and the upper chord are relatively large, so these parts can become potential earthquake-resistant weak parts.

(3) Under multidimensional ground motion excitation, the distribution laws of the maximum absolute axial forces at upper and lower chords of arch rib are obviously

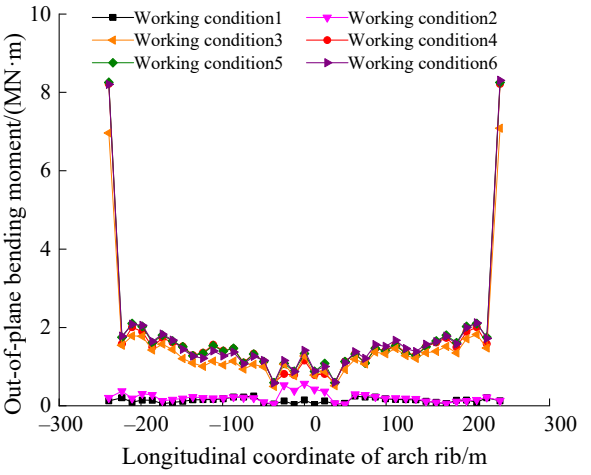

Figure 8.
Out-of-plane bending moment of lower chord of arch rib

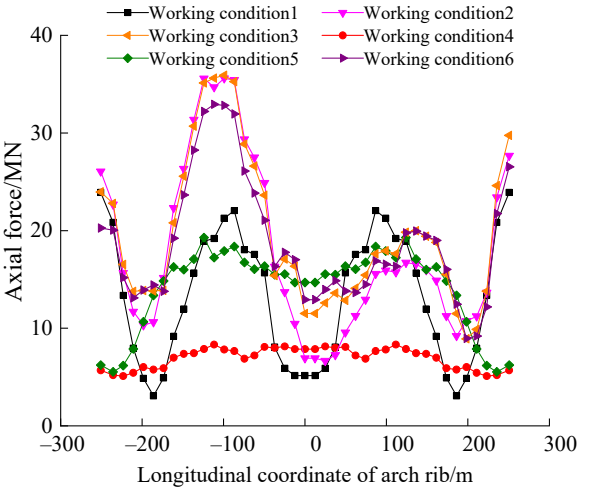

Figure 9.
Axial force of upper chord of arch rib

different. The maximum axial force of the upper chord is distributed as an asymmetric harmonic function, but the maximum axial force of the lower chord mainly occurs at the arch foot, and attenuated sharply towards the midspan. It is worth noting that the maximum absolute value of internal force at arch rib chord is also symmetrical under 1D ground motion excitation. However, under multidimensional seismic excitation, even if the structure is symmetrical, the maximum absolute value of axial force of control section at the symmetrical position of arch rib chord is not symmetrical, which is inconsistent with related concepts in structural mechanics. Therefore, when time history response analysis method is adopted to analyze the seismic response of steel truss arch bridge under multidimensional ground motion, several control sections should be selected along the whole arch rib, and corresponding internal forces should be extracted one by one for combined checking.

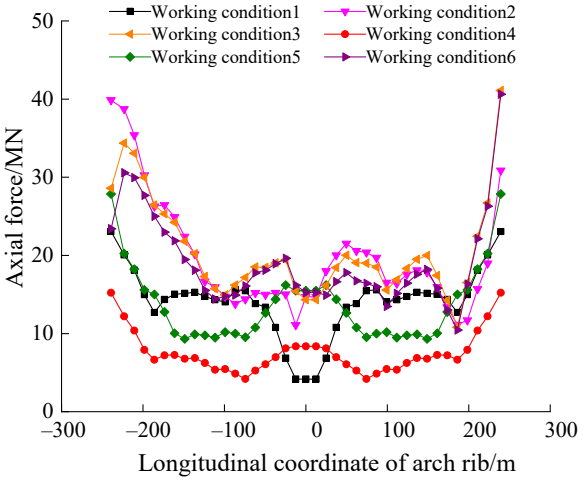

Figure 10.
Axial force of lower chord of arch rib

Member parts	Control section	Axial force ratio		In-plane bending moment ratio		Out-of-plane bending moment ratio	
		Working condition 1	Working condition 2	Working condition 1	Working condition 2	Working condition 1	Working condition 2
Upper chord of arch rib	Left arch foot	1.00	1.09	1.32	1.41	0.09	0.10
	1/4 span	0.54	1.01	0.90	1.02	0.12	0.15
	Arch crown	0.45	0.60	1.03	1.03	0.65	0.67
	3/4 span	0.95	0.84	0.82	0.95	0.12	0.21
	Right arch foot	0.80	0.93	0.73	0.91	0.08	0.10
Lower chord of arch rib	Left arch foot	0.81	1.39	1.41	1.73	0.02	0.03
	1/4 span	0.85	0.96	0.81	1.13	0.16	0.2
	Arch crown	0.29	1.03	0.12	0.59	0.12	0.44
	3/4 span	0.80	0.96	0.66	0.87	0.12	0.15
	Right arch foot	0.56	0.75	0.58	0.74	0.02	0.02

Table 4.
Internal force ratio of control section of arch rib

(4) As the spatial coupling effect of the structure and the maximum internal force response of arch rib under single-dimensional excitation in all directions do not necessarily occur synchronously, the more excitation dimensions at the same time of seismic motion does not necessarily mean the greater internal force of section of main arch rib chord. When multidimensional ground motion is synchronously excited, and if the internal force responses of arch rib under 1D excitation in all directions are synchronous and of the same sign (positive or negative), the internal force response of arch rib under multidimensional excitation is greater than that under single-dimensional excitation. On the contrary, if the internal force responses of arch rib in all directions are in different signs (positive and negative) under 1D excitation, the internal force response of arch rib under multidimensional excitation is smaller than

Member parts	Control section	Axial force ratio		In-plane bending moment ratio		Out-of-plane bending moment ratio	
		Working condition 4	Working condition 5	Working condition 4	Working condition 5	Working condition 5	Working condition 4
Upper chord of arch rib	Left arch foot	0.28	0.31	0.65	0.84	1.02	1.02
	1/4 span	0.24	0.60	0.27	0.38	0.99	1.00
	Arch crown	0.61	1.14	0.09	0.18	0.71	0.71
	3/4 span	0.40	0.98	0.24	0.33	0.98	0.99
	Right arch foot	0.21	0.23	0.29	0.38	0.98	0.98
Lower chord of arch rib	Left arch foot	0.65	1.19	1.27	1.39	1.00	1.01
	1/4 span	0.40	0.63	0.31	0.69	1.12	1.10
	Arch crown	0.55	1.01	0.48	0.98	0.82	0.94
	3/4 span	0.38	0.59	0.23	0.51	0.93	0.91
	Right arch foot	0.37	0.69	0.55	0.60	0.99	0.99

Table 5.
Internal force ratio of control section of arch rib

those under 1D excitation. Generally speaking, the analysis results of 2D and 3D excitation are obviously larger than those of 1D excitation. It is suggested that 2D and 3D ground motion excitation should be carried out simultaneously for complex steel truss arch bridge to determine its most unfavorable response.

The asymmetry of internal force distribution of arch rib chord in the above article (3) is explained as follows. Taking the axial force response of the upper chord of arch rib at ±124 m as an example when the EL-centro wave is input, the axial force time history curves (including the peak value of axial force response in the time period) of the first 10 s under 1D excitation in X and Z directions are as shown in Figures 11 and 12. It can be seen from the figures that the axial force time history curves of upper chord of arch rib at ±124 m under

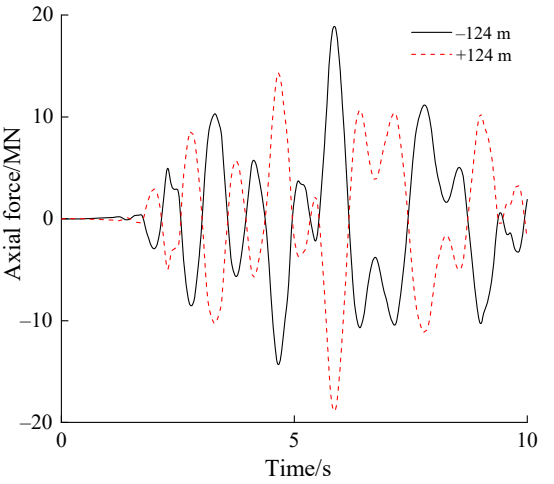

Figure 11.
Time history curve of axial force of upper chord of section at ± 124 m under X-direction excitation

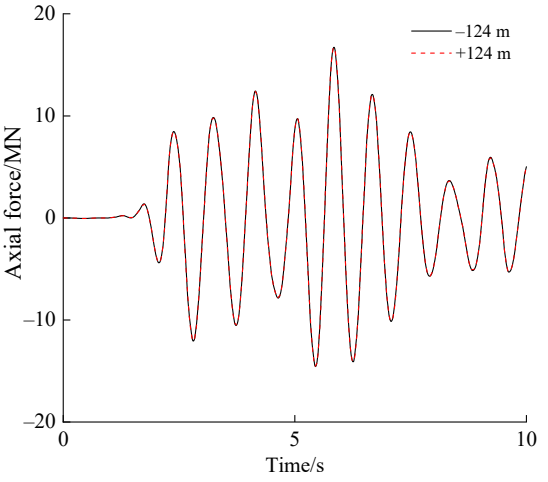

Figure 12.
Time history curve of axial force of upper chord of section at ± 124 m under *Z*-direction excitation

X-direction and *Z*-direction excitation present antisymmetric and positive-symmetric characteristics, respectively (i.e. the axial force properties are different), while the maximum axial force of the upper chord of arch rib should be algebraically superimposed according to corresponding time history curves of axial force under 2D excitation in *X* direction + *Z* direction, which ultimately leads to asymmetric axial force distribution of upper chord of arch rib.

The relationship between the maximum internal force of arch rib chord and the excitation dimension in the above (4) is explained as follows. Taking the axial force responses of the left and right arch feet of the upper chord of arch rib as an example when EL-centro wave is input, the time history curves of axial force in the first 10 seconds (including the peak value of axial force response in the time period) under different ground motion excitation modes are as shown in Figures 13 and 14. It can be seen from Figure 13 that the axial force response peak of the upper chord at the left arch foot occurs at the same time (6.90 s) under 1D excitation in *X* and *Z* directions, but the axial force properties are different. Meanwhile, the axial force

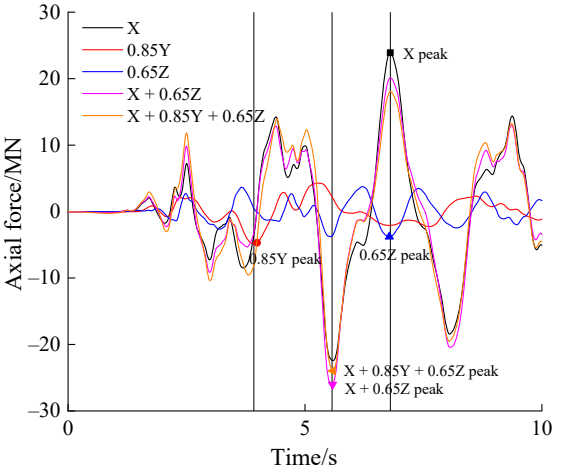

Figure 13.
Time history curve of axial force of upper chord at left arch foot

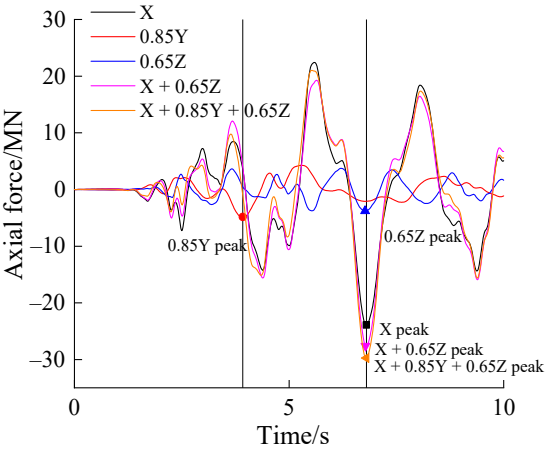

Figure 14.
Time history curve of axial force of upper chord at right arch foot

response of the upper chord under *Y*-direction excitation and the response peak under *X*-direction excitation are also in different signs (positive and negative), which makes the axial forces offset each other, so the axial force response of the upper chord at the left arch foot under 3D excitation is not the largest. It can be seen from Figure 14 that axial force response peak of the upper chord at the right arch foot occurs at the same time (6.90 s) under 1D excitation in *X* and *Z* directions, and the axial force properties are same, while the axial force response of the upper chord under excitation in *Y* direction is of the same sign (positive or negative), as the peaks in *X* and *Z* directions at this time, resulting in the cumulative amplification of axial force. Therefore, the axial force response of the upper chord at the right arch foot is the largest under 3D excitation.

5. Control component of internal force of arch rib chord under 3D excitation

For the long-span deck type steel truss arch bridge, due to the obvious spatial coupling effect, six internal force components can be generated in chord under multidimensional excitation. Among them, the internal force components that produce normal stress in chord section mainly include axial force, in-plane bending moment and out-of-plane bending moment. The normal stress component of chord section is taken as the observation object, the EL-centro wave is taken as the input ground motion, and the ground motion excitation mode is adopted under working condition 6. The distribution of normal stress caused by each internal force component of upper and lower chords along the arch rib is shown in Figures 15 and 16.

It can be seen from Figures 15 and 16 that for the lower chord of arch rib, the normal stress caused by axial force is significantly greater than that caused by in-plane bending moment and out-of-plane bending moment, that is, for the lower chord of arch rib, the axial force is an internal force component that plays an absolute control role, which is the same as the stress characteristics of truss structure. However, according to the magnitude and distribution characteristics of the normal stress of the whole upper chord, it is difficult to find the internal force component that plays an absolute control role, which is obviously different from the stress characteristics of truss structure. The normal stress caused by in-plane bending moment at arch crown, arch foot and the joint between spandrel column and arch rib is large. Especially at arch crown, the normal stress caused by in-plane bending moment is more than four times of that caused by axial force, which shows that the normal stress of the upper chord of arch rib is jointly controlled by axial force, in-plane and out-of-plane bending

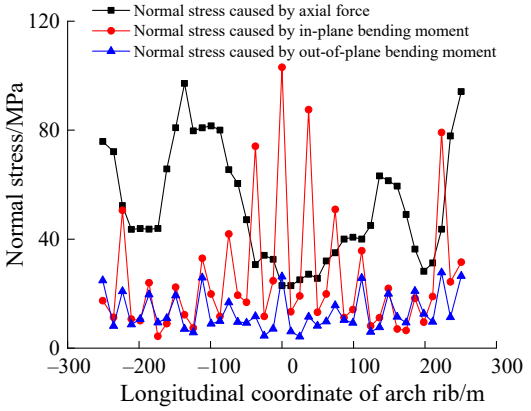

Figure 15.
Normal stress distribution of upper chord of arch rib

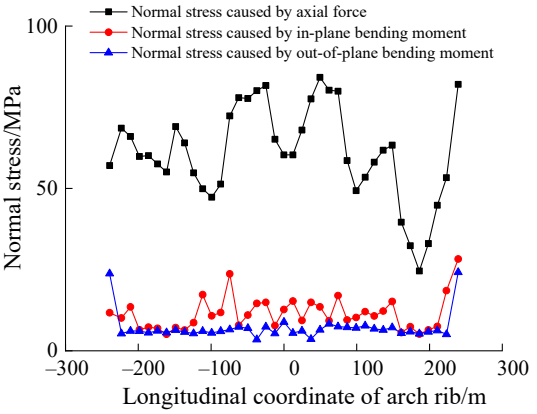

Figure 16.
Normal stress distribution of lower chord of arch rib

moments. The significance of discussing the internal force components controlled by chord is that it can provide reference for qualitative adjustment of section size of chord members: if the bending moment of chord member is large, the normal stress of adjusting section height changes significantly; if the axial force of the chord member is large, the cross-sectional area can be adjusted and attention should be paid to the overall stability.

6. Conclusion

For a steel truss arch bridge composed of multiple arch ribs, any unidirectional ground motion excitation will cause large axial force in the chords of arch rib. The axial force caused by transverse and vertical ground motion excitation in the chords of arch crown area is 1.4–3.6 times of corresponding axial force under longitudinal ground motion excitation, and the in-plane bending moment caused by the lower chord at arch crown is 4.2–5.5 times of corresponding bending moment under longitudinal ground motion excitation.

For the lower chord of arch rib, the arch foot is the earthquake-resistant weak part, but for the upper chord of arch rib, the arch foot, the arch crown and the intersection of the spandrel column may become potential earthquake-resistant weak part.

The in-plane bending moment and out-of-plane bending moment of upper chord of arch rib present obvious multi-peak distribution characteristics along longitudinal direction, and each peak point of bending moment corresponds to the position of column. The maximum in-plane and out-of-plane bending moments of the upper chord of arch rib occur at the arch crown, while the maximum in-plane and out-of-plane bending moments of the lower chord of arch rib occur at the arch foot.

Under multidimensional ground motion excitation, the distribution laws of the maximum absolute values of axial force at upper and lower chords of arch rib are different. The maximum axial force of the upper chord is distributed as an asymmetric harmonic function, while the maximum axial force of the lower chord occurs at the arch foot, and attenuated sharply towards the midspan.

When time history response analysis method is adopted to analyze the seismic response of long-span steel truss arch bridge under 2D or 3D ground motion excitation mode, several control sections should be selected along the whole arch rib, and corresponding internal forces should be extracted one by one for combined checking. It is suggested that 2D and 3D ground motion excitation should be carried out simultaneously for long-span steel truss arch bridge to determine the most unfavorable response.

Under 3D ground motion excitation, the normal stress of the lower chord of arch rib is mainly caused by axial force; the normal stress of the upper chord of arch rib is jointly caused by axial force, in-plane and out-of-plane bending moments. In the area ±50 m away from the arch crown section, the normal stress caused by in-plane bending moment in the chord at the joint between the spandrel column and the arch rib is larger.

References

Chen, D., & Guo, W. (2010). Spatial seismic response analysis of long-span steel truss arch bridge. *Journal of Central South University (Natural Science)*, *41*(4), 1590–1596.

Chen, X., & Xia, X. (2018). Study on ground motion input mode of long-span arch bridge. *World Earthquake Engineering*, *34*(2), 26–32.

European Committee for Standardization (2005). *EN 1998-2: 2005 Eurocode 8-design of Structures for Earthquake Resistance Part 2: Bridges*. Bruxelles: European Committee for Standardization (CEN).

Fan, L. (1990). *Aseismic design of bridges*. Shanghai: Tongji University Press.

Li, X., Hong, Q., Lei, H., & Liu, Z. H. (2015). Effect of input directions of seismic ground motion on seismic responses of a railway extradosed bridge. *Bridge Construction*, *45*(1), 26–32.

Li, X., Liu, M., Yang, D., Dai, S. H., & Xiao, L. (2020). Seismic damage evolution simulation of long-span deck steel truss arch bridge. *Journal of Southwest Jiaotong University*, *55*(6), 1207–1214.

Liang, Z., & Chen, A. (2009). Earthquake seismic analysis of long span steel deck arch bridge considering effects of elasto-plastic finite displacement. *Journal of Vibration and Shock*, *28*(11), 139–145.

Luo, H., Zhu, D., & Yu, J. (2019). Seismic response characteristics of a rib arch bridge. *Journal of Chongqing Jiaotong University (Natural Science)*, *38*(6), 30–36.

Peng, Y., Zhu, D., & Zang, B. (2009). Vertical seismic response on a top-bear arch bridge. *Journal of Chongqing Jiaotong University (Natural Science)*, *28*(3), 475–479.

Su, C., & Chen, H. (2008). Seismic response of long-span bridge under multi-support excitation. *Journal of South China University of Technology (Natural Science Edition)*, *36*(11), 101–107.

Wang, K., & Li, Q. (2007). Research progress on aseismic design of bridges. *Engineering Mechanics*, *24*(September 2), 75–82.

Xia, C., & Zhong, T. (2009). Seismic response analysis on Nanjing Dashengguan Yangtze River bridge of high-speed railway. *China Railway Science*, *30*(5), 39–45.

Zhao, C., & Zhou, Z. (2006). Seismic response analysis of long-span steel braced deck-type arch bridge. *Journal of Railway Science and Engineering*, *5*(3), 6–11.

Zhao, C., & Zhou, Z. (2007). Seismic response analysis of long-span CFST deck-type arch bridge. *Journal of Chongqing Jiaotong University (Natural Science)*, *26*(5), 120–4.

Zhuge, H., Xie, X., Liao, Y., & Tang, Z. H. (2019). Effect of transverse earthquake action on development of seismic damage of steel arch bridges. *Journal of Zhejiang University (Engineering Science)*, *53*(4), 702–712.

Further reading

Ministry of Housing and Urban-Rural Development of the People's Republic of China (2016). *GB 50011-2010 code for seismic design of buildings*. Beijing: China Construction Industry Press.

The Ministry of Railways of the People's Republic of China (2006). *GB 50111—2006 Code for Seismic Design of Railway Engineering*. Beijing: China Planning Press.

Corresponding author

Yongliang Zhang can be contacted at: zhangyong_L@126.COM